On Time-Delay Estimation Accuracy Limit Under Phase Uncertainty

1st Joan M. Bernabeu
ISAE-SUPAERO, TéSA
University of Toulouse
Toulouse, France
joan.bernabeu@tesa.prd.fr

2nd Lorenzo Ortega
IPSA, TéSA
Toulouse, France
lorenzo.ortega@ipsa.fr

3rd Antoine Blais
ENAC
University of Toulouse
Toulouse, France
blais@recherche.enac.fr

4th Yoan Grégoire
CNES
Toulouse, France
yoan.gregoire@cnes.fr

5th Eric Chaumette
ISAE-SUPAERO
University of Toulouse
Toulouse, France
eric.chaumette@isae-supaero.fr

***Abstract*—Accurately determining signal time-delay is crucial across various domains, such as localization and communication systems. Understanding the achievable optimal estimation performance of such technologies, especially during design phases, is essential for benchmarking purposes. One common approach is to derive bounds like the Cramér-Rao Bound (CRB), which directly reflects the minimum achievable estimation error for unbiased estimators. Different studies vary in their approach to deal with the degree of misalignment in the global phase originating from both the transmitter and the receiver in a single input, single output (SISO) link during time-delay estimation assessment. While some treat this phase term as unknown, others assume ideal calibration and compensation. As an alternative to these two opposing approaches, this study adopts a more balanced approach by considering that such a phase can be estimated with a defined uncertainty, a measure that could be implemented in many practical applications. The primary contribution provided lies in the derivation of a closed-form CRB expression for this alternative signal model, which, as observed, exhibits an asymptotic behavior transitioning between the results observed in previous studies, influenced by the uncertainty assumed for the mentioned phase term.**

***Index Terms*—Cramér-Rao bound, time-delay and phase estimation, band-limited signals.**

I. Introduction

Time-delay estimation is a field of study with widespread applications across multiple domains [1]–[3], as it provides valuable insights into the propagation of a signal through different mediums. For some applications it constitutes a fundamental component, such as in localization via Global Navigation Satellite Systems [4] [5], direction of arrival estimation in array processing [6] [7] or synchronization in communication [8] . For this reason, it is imperative to possess an understanding of the attainable optimal estimation performance of such technologies, particularly during the design phases, where such knowledge may serve as an indicator of feasibility. A common approach followed in the state of the art is to derive the Cramér-Rao Bound (CRB) [9] to bound the variance in the estimation, which equals the mean-squared error (MSE) for unbiased estimators [9]. The CRB is a well established statistical tool which provides a simple and effective way to formulate an expression that bounds the MSE of unbiased estimators [10], [11]. Depending on whether the relative distance in a transmitter-to-receiver link is static or dynamic, it may be necessary to take into account the Doppler effect in the estimation of the time-delay. It is the reason why numerous CRBs expressions have been derived for the time-delay τ and Doppler frequency b estimation considering parametric narrow-band signal models, for instance [12]–[16], making emphasis on time-delay estimation, and regarding the Doppler frequency as a nuisance parameter [9] requiring estimation for its compensation. Most of these studies include a phase term $\phi = \psi + w_c\tau$, which combines a phase component ψ, representing the degree of misalignment in the global phase originating from both the transmitter and the receiver, with the phase term $w_c\tau$ attributable to the wave propagation process. Since both terms cannot a priori be distinguished one from another, studies adopt two main strategies to model ϕ. On the one hand, as in [17], [18], most of the existing studies propose to group ϕ into the signal's amplitude α, turning the latter into a complex parameter. On the other hand, as in [19], [20], ψ is assumed to be perfectly calibrated and compensated, giving way to the inclusion of $w_c\tau$ in theoretical derivations. As an alternative to these two opposing approaches, this study adopts a more balanced approach that could be implemented in many practical applications. Indeed, rather than assuming perfect calibration of ψ, it considers a scenario where it is estimated with a certain level of uncertainty, akin to real-world conditions where calibration steps can provide measurements up to a certain level of precision.

In that perspective, the primary contribution provided lies in the derivation of a closed-form CRB expression for this alternative signal model, which, as observed, exhibits an asymptotic behavior transitioning between the results observed

This work was partially supported by CNES, IPSA and DGA/AID project 2021.65.0070.

in previous studies, influenced by the uncertainty assumed for the mentioned phase term.

This communication is organized into three main sections. Firstly, Section II introduces the use-case scenario, the assumed band-limited signal model, and the notation used. Following that, Section III offers the derivation of the CRB associated to general signal model accounting for both the time-delay and the Doppler effect. Then, it introduces a simplification by disregarding the Doppler effect, and provides two cases of interest for the resulting expressions. Subsequently, Section IV outlines the tests conducted to validate the previously derived CRBs, along with providing remarks based on the observed results. Finally, Section V provides a summary of the main points of this contribution, highlighting the key observations.

II. Signal Model

The signal model utilized in this manuscript is based on the well-known conditional signal model (CSM) [10], [11], and it is formulated according to previous contributions in the same topic [21]–[24]. Hence, as detailed in [20], the received band-limited signal after the Hilbert filter can be expressed as,

$$x(t) = \left(\alpha e^{j\phi}\right) c(t;\boldsymbol{\eta}) e^{-jw_c b(t-\tau)} + n(t), \tag{1}$$

where $\boldsymbol{\eta}^T = (\tau, b)$, $\phi = \psi + w_c\tau$, $\alpha \in \mathbb{R}^+$ is the signal's amplitude and $n(t)$ a complex zero-mean additive white Gaussian noise (AWGN), and $c(t)$ is the base-band signal. This study assumes parameter ψ to be estimated. Thus, (1) becomes,

$$x(t) = \alpha \mathbf{a}(t;\boldsymbol{\eta}) + n(t), \quad n(t) \sim \mathcal{CN}(0, \sigma_n^2), \tag{2}$$

where $\mathbf{a}(t;\boldsymbol{\eta}) = c(t)e^{j\psi}e^{\varphi(t;\boldsymbol{\eta})}$, and $\varphi(t;\boldsymbol{\eta}) = -jw_c(\tau + b(t-\tau))$, with $w_c = 2\pi \mathrm{F_c}$. Moreover, in addition to (2), it is assumed the availability of ψ_a as a sensor measurement of the true phase offset ψ, modeled as a stochastic variable following a normal probability distribution function (PDF) with a degree of uncertainty given by the variance σ_a^2,

$$\psi_a(t) = \psi + n_a(t), \quad n_a(t) \sim \mathcal{N}(0, \sigma_{n_a}^2). \tag{3}$$

The discrete-time signal model representation considers the acquisition of $N' = N_2' - N_1' + 1$ samples from (2). To ensure operation under the asymptotic regime it is assumed that $N_1' \ll N_1$, $N_2' \gg N_2$. The associated sampling rate is $\mathrm{T_s} = 1/\mathrm{F_s}$, and $\mathrm{F_s} \geq B$, B being the signal's bandwidth. This is,

$$\mathbf{x} = \alpha\mathbf{a}(\boldsymbol{\eta}) + \mathbf{n},\ \mathbf{x} = \begin{pmatrix} x(N_1'\mathrm{T_s}) \\ \vdots \\ x(N_2'\mathrm{T_s}) \end{pmatrix},\ \mathbf{n} = \begin{pmatrix} n(N_1'\mathrm{T_s}) \\ \vdots \\ n(N_2'\mathrm{T_s}) \end{pmatrix}, \tag{4}$$

and,

$$\mathbf{a}(\boldsymbol{\eta}) = \begin{pmatrix} c\left(N_1'\mathrm{T_s} - \tau\right) e^{-jw_c(\tau + b(N_1'\mathrm{T_s} - \tau))} \\ \vdots \\ c\left(N_2'\mathrm{T_s} - \tau\right) e^{-jw_c(\tau + b(N_2'\mathrm{T_s} - \tau))} \end{pmatrix} e^{\psi}. \tag{5}$$

where $\mathbf{n} \sim \mathcal{CN}(0, \sigma_n^2 \mathbf{I}_{N'})$. The set of unknown parameters to be estimated are

$$\boldsymbol{\epsilon}^T = (\sigma_n^2, \boldsymbol{\zeta}^T), \quad \boldsymbol{\zeta}^T = (\alpha, \boldsymbol{\theta}^T), \quad \boldsymbol{\theta}^T = (\psi, \boldsymbol{\eta}^T), \tag{6}$$

being τ and b, the time-delay and Doppler frequency, respectively.

III. Cramér Rao Bound

The signal models in (2) and (3) represent the combination of two Gaussian PDFs; one stemming from the additive noise $n(t)$, and another from the measurement ψ_a. This contribution formulates the CRB expression by deriving the associated Fisher Information Matrix (FIM) [25]. For this particular use-case, the FIM for the vector of unknown parameters $\boldsymbol{\epsilon}$, denoted as $\mathbf{F}(\boldsymbol{\epsilon})$, is derived considering a joint PDF from both $x(t)$ and ψ_a;

$$p(x, \psi_a; \boldsymbol{\epsilon}) = p(x; \boldsymbol{\epsilon}) p(\psi_a; \psi), \tag{7}$$

which results in:

$$\begin{aligned} \mathbf{F}(\boldsymbol{\epsilon}) &= \\ &= \mathrm{E}\left\{ \frac{\partial^2 \ln(p(\mathbf{x}, \psi_a; \boldsymbol{\epsilon}))}{\partial\boldsymbol{\epsilon}\partial\boldsymbol{\epsilon}^T} \right\}, \\ &= \mathrm{E}\left\{ \frac{\partial^2 \left(\ln p(\mathbf{x}; \boldsymbol{\epsilon}) + \ln p(\psi_a; \psi) \right)}{\partial\boldsymbol{\epsilon}\partial\boldsymbol{\epsilon}^T} \right\}, \\ &= \mathrm{E}\left\{ \frac{\partial^2 \ln p(\mathbf{x}; \boldsymbol{\epsilon})}{\partial\boldsymbol{\epsilon}\partial\boldsymbol{\epsilon}^T} \right\} + \mathrm{E}\left\{ \frac{\partial^2 \ln p(\psi_a; \psi))}{\partial\boldsymbol{\epsilon}\partial\boldsymbol{\epsilon}^T} \right\}, \\ &= \mathbf{F}(\mathbf{x}, \boldsymbol{\epsilon}) + \mathbf{F}(\psi), \end{aligned} \tag{8}$$

with $\mathrm{E}\{\cdot\}$ being the expectation operator. The FIM can be conveniently obtained in both cases by applying the Slepian-Bangs formula [26] for each unknown parameter in $\boldsymbol{\epsilon}$, since the two PDFs involved are Gaussian. Hence,

$$\mathbf{F}(\boldsymbol{\zeta}) = \begin{bmatrix} F(\alpha) & [F(\alpha,\psi), \mathbf{F}(\alpha, \boldsymbol{\eta}^T)] \\ \begin{bmatrix} F(\psi,\alpha) \\ \mathbf{F}(\boldsymbol{\eta},\alpha) \end{bmatrix} & \mathbf{F}(\boldsymbol{\theta}) \end{bmatrix}, \tag{9a}$$

with,

$$\mathbf{F}(\boldsymbol{\theta}) = \begin{bmatrix} F(\psi) & \mathbf{F}(\psi, \boldsymbol{\eta}^T) \\ \mathbf{F}(\boldsymbol{\eta}, \psi) & \mathbf{F}(\boldsymbol{\eta}) \end{bmatrix}, \tag{9b}$$

and,

$$\mathbf{F}(\boldsymbol{\eta}) = \begin{bmatrix} F(\tau) & F(\tau, b) \\ F(b, \tau) & F(b) \end{bmatrix}, \tag{9c}$$

are explictly given by[1]

$$\mathbf{F}(\boldsymbol{\zeta}) = \frac{2}{\sigma_n^2} \begin{bmatrix} \|\mathbf{a}(\boldsymbol{\eta})\|^2 & \left[0, \alpha\Re\left\{ \mathbf{a}(\boldsymbol{\eta})^H \frac{\partial \mathbf{a}(\boldsymbol{\eta})}{\partial \boldsymbol{\eta}^T} \right\}\right] \\ \begin{bmatrix} 0 \\ \alpha\Re\left\{ \mathbf{a}(\boldsymbol{\eta})^H \frac{\partial \mathbf{a}(\boldsymbol{\eta})}{\partial \boldsymbol{\eta}^T} \right\}^T \end{bmatrix} & \mathbf{F}(\boldsymbol{\theta}) \end{bmatrix}, \tag{10a}$$

[1]Note that $\Re\{\cdot\}$ and $\Im\{\cdot\}$ represent the real and imaginary part operators, respectively.

with,

$$\mathbf{F}(\boldsymbol{\theta}) = \begin{bmatrix} \|\mathbf{a}(\boldsymbol{\eta})\|^2\alpha^2 + \frac{\sigma_n^2}{2}\frac{1}{\sigma_{n_a}^2} & \alpha^2\Im\left\{\mathbf{a}(\boldsymbol{\eta})^H\frac{\partial\mathbf{a}(\boldsymbol{\eta})}{\partial\boldsymbol{\eta}^T}\right\} \\ \alpha^2\Im\left\{\mathbf{a}(\boldsymbol{\eta})^H\frac{\partial\mathbf{a}(\boldsymbol{\eta})}{\partial\boldsymbol{\eta}^T}\right\}^T & \alpha^2\Re\left\{\left(\frac{\partial\mathbf{a}(\boldsymbol{\eta})}{\partial\boldsymbol{\eta}^T}\right)^H\frac{\partial\mathbf{a}(\boldsymbol{\eta})}{\partial\boldsymbol{\eta}^T}\right\} \end{bmatrix}, \tag{10b}$$

where the squared-matrix arrangement in (10a) facilitates the operations towards a closed-form for $\mathbf{CRB}_{\boldsymbol{\eta}}$ which is the primary goal of this study. For this, the first step consists in computing $\mathbf{CRB}_{\boldsymbol{\theta}}$ which contains $\mathbf{CRB}_{\boldsymbol{\eta}}$. The inverse of $\mathbf{F}(\boldsymbol{\zeta})$ can be formulated by means of the block matrix inversion lemma [27]. Considering the following matrix arrangement,

$$\begin{aligned}\mathbf{F}(\boldsymbol{\zeta})^{-1} &= \begin{bmatrix}\mathbf{A}_{11} & \mathbf{A}_{12}\\ \mathbf{A}_{21} & \mathbf{A}_{22}\end{bmatrix}^{-1} \\ &= \begin{bmatrix}\mathbf{A}_{11}^{-1} + \mathbf{A}_{11}^{-1}\mathbf{A}_{12}\mathbf{C}_2^{-1}\mathbf{A}_{21}\mathbf{A}_{11}^{-1} & \mathbf{A}_{11}^{-1}\mathbf{A}_{12}\mathbf{C}_2^{-1}\\ \mathbf{C}_2^{-1}\mathbf{A}_{21}\mathbf{A}_{11}^{-1} & \mathbf{C}_2^{-1}\end{bmatrix}, \end{aligned} \tag{11}$$

$\mathbf{CRB}_{\boldsymbol{\theta}}$ is calculated as,

$$\mathbf{CRB}_{\boldsymbol{\theta}} \equiv \mathbf{C}_2^{-1} = (\mathbf{A}_{22} - \mathbf{A}_{21}\mathbf{A}_{11}^{-1}\mathbf{A}_{12})^{-1}, \tag{12}$$

which results in

$$\mathbf{CRB}_{\boldsymbol{\theta}}^{-1} = \frac{2\alpha^2}{\sigma_n^2}\begin{bmatrix} \|\mathbf{a}(\boldsymbol{\eta})\|^2 + \frac{\sigma_n^2}{2}\frac{1}{\sigma_{n_a}^2} & \Im\left\{\mathbf{a}(\boldsymbol{\eta})^H\frac{\partial\mathbf{a}(\boldsymbol{\eta})}{\partial\boldsymbol{\eta}^T}\right\} \\ \Im\left\{\mathbf{a}(\boldsymbol{\eta})^H\frac{\partial\mathbf{a}(\boldsymbol{\eta})}{\partial\boldsymbol{\eta}^T}\right\}^T & \mathbb{F}(\boldsymbol{\eta}) \end{bmatrix} \tag{13}$$

with

$$\begin{aligned}\mathbb{F}(\boldsymbol{\eta}) = \Re\left\{\left(\frac{\partial\mathbf{a}(\boldsymbol{\eta})}{\partial\boldsymbol{\eta}^T}\right)^H\frac{\partial\mathbf{a}(\boldsymbol{\eta})}{\partial\boldsymbol{\eta}^T}\right\} \\ - \frac{\Re\left\{\mathbf{a}(\boldsymbol{\eta})^H\frac{\partial\mathbf{a}(\boldsymbol{\eta})}{\partial\boldsymbol{\eta}^T}\right\}^T\Re\left\{\mathbf{a}(\boldsymbol{\eta})^H\frac{\partial\mathbf{a}(\boldsymbol{\eta})}{\partial\boldsymbol{\eta}^T}\right\}}{\|\mathbf{a}(\boldsymbol{\eta})\|^2}.\end{aligned} \tag{14}$$

The block matrix inversion lemma is applied again, as in (12), to yield the expression for $\mathbf{CRB}_{\boldsymbol{\eta}}$

$$\begin{aligned}\mathbf{CRB}_{\boldsymbol{\eta}} = \frac{\sigma_n^2}{2\alpha^2}\Bigg(\Re\left\{\left(\frac{\partial\mathbf{a}(\boldsymbol{\eta})}{\partial\boldsymbol{\eta}^T}\right)^H\frac{\partial\mathbf{a}(\boldsymbol{\eta})}{\partial\boldsymbol{\eta}^T}\right\} \\ - \frac{\Re\left\{\mathbf{a}(\boldsymbol{\eta})^H\frac{\partial\mathbf{a}(\boldsymbol{\eta})}{\partial\boldsymbol{\eta}^T}\right\}^T\Re\left\{\mathbf{a}(\boldsymbol{\eta})^H\frac{\partial\mathbf{a}(\boldsymbol{\eta})}{\partial\boldsymbol{\eta}^T}\right\}}{\|\mathbf{a}(\boldsymbol{\eta})\|^2} \\ - \frac{\Im\left\{\mathbf{a}(\boldsymbol{\eta})^H\frac{\partial\mathbf{a}(\boldsymbol{\eta})}{\partial\boldsymbol{\eta}^T}\right\}^T\Im\left\{\mathbf{a}(\boldsymbol{\eta})^H\frac{\partial\mathbf{a}(\boldsymbol{\eta})}{\partial\boldsymbol{\eta}^T}\right\}}{\|\mathbf{a}(\boldsymbol{\eta})\|^2} \\ + \frac{\Im\left\{\mathbf{a}(\boldsymbol{\eta})^H\frac{\partial\mathbf{a}(\boldsymbol{\eta})}{\partial\boldsymbol{\eta}^T}\right\}^T\Im\left\{\mathbf{a}(\boldsymbol{\eta})^H\frac{\partial\mathbf{a}(\boldsymbol{\eta})}{\partial\boldsymbol{\eta}^T}\right\}}{\|\mathbf{a}(\boldsymbol{\eta})\|^2(1+2\sigma_{n_a}^2\mathrm{SNR}_{\text{out}})}\Bigg)^{-1}.\end{aligned} \tag{15}$$

Considering the following relationships,

$$\Re\{\mathbf{A}^H\mathbf{A}\} = \Re\{\mathbf{A}\}^T\Re\{\mathbf{A}\} + \Im\{\mathbf{A}\}^T\Im\{\mathbf{A}\}, \tag{16}$$

equation (15) can be further derived into,

$$\begin{aligned}\mathbf{CRB}_{\boldsymbol{\eta}} = \frac{\sigma_n^2}{2\alpha^2}\Bigg(\Re\left\{\left(\frac{\partial\mathbf{a}(\boldsymbol{\eta})}{\partial\boldsymbol{\eta}^T}\right)^H\frac{\partial\mathbf{a}(\boldsymbol{\eta})}{\partial\boldsymbol{\eta}^T}\right\} \\ - \frac{\Re\left\{\left(\mathbf{a}(\boldsymbol{\eta})^H\frac{\partial\mathbf{a}(\boldsymbol{\eta})}{\partial\boldsymbol{\eta}^T}\right)^H\left(\mathbf{a}(\boldsymbol{\eta})^H\frac{\partial\mathbf{a}(\boldsymbol{\eta})}{\partial\boldsymbol{\eta}^T}\right)\right\}}{\|\mathbf{a}(\boldsymbol{\eta})\|^2} \\ + \frac{\Im\left\{\mathbf{a}(\boldsymbol{\eta})^H\frac{\partial\mathbf{a}(\boldsymbol{\eta})}{\partial\boldsymbol{\eta}^T}\right\}^T\Im\left\{\mathbf{a}(\boldsymbol{\eta})^H\frac{\partial\mathbf{a}(\boldsymbol{\eta})}{\partial\boldsymbol{\eta}^T}\right\}}{\|\mathbf{a}(\boldsymbol{\eta})\|^2(1+2\sigma_{n_a}^2\mathrm{SNR}_{\text{out}})}\Bigg)^{-1}.\end{aligned} \tag{17}$$

The derivative terms in (17) are provided as a function of (2), to facilitate subsequent calculations;

$$\frac{\partial\mathbf{a}(t;\boldsymbol{\eta})}{\partial\boldsymbol{\eta}^T} = \left(\frac{\partial\mathbf{a}(t;\boldsymbol{\eta})}{\partial\tau}, \quad \frac{\partial\mathbf{a}(t;\boldsymbol{\eta})}{\partial b}\right) = -\mathbf{Q}\mathbf{v}(t;\boldsymbol{\eta})\,e^{\psi} \tag{18}$$

where,

$$\mathbf{Q} = -\begin{bmatrix} jw_c(1-b) & 0 & 1 \\ 0 & jw_c & 0\end{bmatrix}, \tag{19}$$

$$\mathbf{v} = \begin{bmatrix} c(t), & (t-\tau)c(t), & c^{(1)}(t)\end{bmatrix}^T. \tag{20}$$

With this decomposition and assuming a band-limited signal, a closed-form expression of the $\mathbf{CRB}_{\boldsymbol{\eta}}$ can be derived via the Nyquist-Shannon theorem [28], applied to the discrete-time signal model in (4). Indeed,

$$\begin{aligned}\lim_{(N_1',N_2')\to(-\infty,\infty)} \mathrm{T_s}\sum_{n=N_1'}^{N2'}\mathbf{v}(n\mathrm{T_s};\boldsymbol{\eta})\,\mathbf{v}^{\mathrm{H}}(n\mathrm{T_s};\boldsymbol{\eta}) \\ = \int_{-\infty}^{\infty}\mathbf{v}(t)\,\mathbf{v}^{\mathrm{H}}(t)\,dt = \mathbf{W},\end{aligned} \tag{21}$$

$$\begin{aligned}\lim_{(N_1',N_2')\to(-\infty,\infty)} T_s\sum_{n=N_1'}^{N2'}\mathbf{v}(n\mathrm{T_s};\boldsymbol{\eta})a^*(n\mathrm{T_s};\boldsymbol{\eta}) \\ = \int_{-\infty}^{\infty}\mathbf{v}(t)a^*(t)\,dt = \mathbf{w},\end{aligned} \tag{22}$$

with,

$$\mathbf{W} = \begin{bmatrix} w_1 & w_2^* & w_3^* & w_4^* \\ w_2 & W_{2,2} & w_4^* & W_{4,2}^* \\ w_3 & w_4 & W_{3,3} & W_{4,3}^* \\ w_4 & W_{4,2} & W_{4,3} & W_{4,4}\end{bmatrix}, \quad \mathbf{w} = \begin{bmatrix} w_1 \\ w_2 \\ w_3 \\ w_4\end{bmatrix}. \tag{23}$$

The following relationships are proved to be useful to reformulate the derivative terms in (17) as,

$$\begin{aligned}\left(\frac{\partial\mathbf{a}(\boldsymbol{\eta})}{\partial\boldsymbol{\eta}^T}\right)^H\frac{\partial\mathbf{a}(\boldsymbol{\eta})}{\partial\boldsymbol{\eta}^T} &= (-\mathbf{Q}\mathbf{v}\,e^{\psi(\boldsymbol{\eta})})^H(-\mathbf{Q}\mathbf{v}\,e^{\psi(\boldsymbol{\eta})}) \\ &= \mathbf{Q}\mathbf{v}\mathbf{v}^H\mathbf{Q}^H \\ &= \mathrm{F_s}\mathbf{Q}\mathbf{W}\mathbf{Q}^H\end{aligned} \tag{24a}$$

$$\begin{aligned}\mathbf{a}(\boldsymbol{\eta})^H\frac{\partial\mathbf{a}(\boldsymbol{\eta})}{\partial\boldsymbol{\eta}^T} &= (a(t;\boldsymbol{\eta})e^{\psi})^H(-\mathbf{Q}\mathbf{v}\,e^{\psi(\boldsymbol{\eta})}) \\ &= -\mathbf{Q}\mathbf{v}\,e^{\psi(\boldsymbol{\eta})}c^H(t;\boldsymbol{\eta}) \\ &= -\mathrm{F_s}(\mathbf{Q}\mathbf{w})^T.\end{aligned} \tag{24b}$$

The expressions in (24) can be included in (17), yielding to:

$$\mathbf{CRB}_{\boldsymbol{\eta}} = \frac{\mathrm{F_s} w_1}{2\mathrm{SNR}_{\text{out}}} \Bigg(\mathrm{F_s} \Re\left\{ \mathbf{QWQ}^H \right\} - \frac{\mathrm{F_s} \Re\left\{ (\mathbf{Qw})^H (\mathbf{Qw}) \right\}^T}{w_1} \tag{25a}$$

$$+ \frac{\mathrm{F_s} \Im\left\{ (\mathbf{Qw})^H (\mathbf{Qw}) \right\}^T}{w_1 (1 + 2\sigma_{n_a}^2 \mathrm{SNR}_{\text{out}})} \Bigg)^{-1}, \tag{25b}$$

where the signal-to-noise ratio (SNR) at the output of the receiver's matched filter $\mathrm{SNR}_{\text{out}}$ [9] for the true parameters α^0 and $\boldsymbol{\eta}^0$, can be determined as,

$$\mathrm{SNR}_{\text{out}} = \left. \frac{\Re\left\{ \left(\frac{\mathbf{a}'(\boldsymbol{\eta})}{\|\mathbf{a}'(\boldsymbol{\eta})\|} \right)^{\mathrm{H}} \left(\alpha^0 \mathbf{a}'\left(\boldsymbol{\eta}^0\right) \right) \right\}^2}{\mathrm{E}\left[\Re\left\{ \left(\frac{\mathbf{a}'(\boldsymbol{\eta})}{\|\mathbf{a}'(\boldsymbol{\eta})\|} \right)^{\mathrm{H}} \mathbf{n} \right\}^2 \right]} \right|_{\boldsymbol{\eta}}$$

$$= \frac{\left(\alpha^0\right)^2 \left\| \mathbf{a}'\left(\boldsymbol{\eta}^0\right) \right\|^2}{\frac{(\sigma_n^0)^2}{2}} = \frac{2\left\|\mathbf{a}\right\|^2}{\left(\sigma_n^0\right)^2} \left(\alpha^0\right)^2 = \frac{2\mathrm{F_s} w_1}{\left(\sigma_n^0\right)^2} \left(\alpha^0\right)^2. \tag{26}$$

Equation (25) presents a squared matrix, which after being inverted provides in its diagonal the asymptotic estimation performance of parameters τ and b. Compared to the results obtained in previous studies on the same topic [17], [21], [22], [24], equation (25) depends not only on $\sigma_n^2, \alpha, \boldsymbol{\eta}$, but also on the uncertainty $\sigma_{n_a}^2$, introduced by the measurement of ψ_a, as denoted in (25b).

Two cases of interest arise after assessing the limits of (25) with respect to $\sigma_{n_a}^2$,

$$\lim_{\sigma_{n_a}^2 \to 0} \mathbf{CRB}_{\boldsymbol{\eta}} = \frac{\mathrm{F_s} w_1}{2\mathrm{SNR}_{\text{out}}} \Bigg(\mathrm{F_s} \Re\left\{ \mathbf{QWQ}^H \right\} - \frac{\mathrm{F_s} \Re\left\{ (\mathbf{Qw})^H (\mathbf{Qw}) \right\}^T}{w_1} + \frac{\mathrm{F_s} \Im\left\{ (\mathbf{Qw})^H (\mathbf{Qw}) \right\}^T}{w_1} \Bigg)^{-1}, \tag{27a}$$

$$\lim_{\sigma_{n_a}^2 \to \infty} \mathbf{CRB}_{\boldsymbol{\eta}} = \frac{\mathrm{F_s} w_1}{2\mathrm{SNR}_{\text{out}}} \Bigg(\mathrm{F_s} \Re\left\{ \mathbf{QWQ}^H \right\} - \frac{\mathrm{F_s} \Re\left\{ (\mathbf{Qw})^H (\mathbf{Qw}) \right\}^T}{w_1} \Bigg)^{-1}. \tag{27b}$$

It is noteworthy that when $\sigma_{n_a}^2 \to 0$, meaning perfect knowledge of ψ_a, (27a) aligns with the expression derived in [19], which assumes perfect knowledge of parameter ψ within its signal model. Conversely, when $\sigma_{n_a}^2 \to \infty$, indicating an inability to infer the ψ parameter, (27b) aligns with the expression derived in [17], where terms ψ and α from (2) were amalgamated and estimated as a single unknown parameter. Thus, the behavior of (25) is expected to fall between the bounds derived in [17] and [19], due to the impact of the product between $\sigma_{n_a}^2$ and $\mathrm{SNR}_{\text{out}}$ defined in (25b).

A. Signal model with known Doppler effect

In certain applications, there may be no requirement to account for the Doppler effect stemming from the dynamics between the transmitter and the receiver. Therefore, the estimation performance evaluations of static scenarios are not influenced by the unknown parameter b. As a consequence, the signal model can be reformulated as,

$$x(t) = \alpha c(t-\tau) e^{j\psi} e^{jw_c\tau} + n(t), \quad n(t) \sim \mathcal{CN}(0, \sigma_n^2). \tag{28}$$

Subsequently, the vector of unknowns reduces to:

$$\boldsymbol{\epsilon} = (\alpha, \sigma_n^2, \boldsymbol{\zeta}), \quad \boldsymbol{\zeta} = (\psi, \eta), \quad \eta = \tau. \tag{29}$$

Notably, η in this case represents a scalar variable. The derivations presented in Section III remain applicable up to the definition of the derivative terms in (18). In this scenario, the definition is reformulated as follows:

$$\frac{\partial \mathbf{a}(t-\tau)}{\partial \tau} = \mathbf{qv}, \tag{30}$$

where,

$$\mathbf{q} = [jw_c, 1], \tag{31}$$

$$\mathbf{v} = [c(t-\tau), c^{(1)}(t-\tau)]^T. \tag{32}$$

These vectors facilitate the reformulation of (17), akin to the process that yields (25). However, now:

$$\mathbf{W} = \begin{bmatrix} w_1 & w_3^* \\ w_3 & W_{3,3} \end{bmatrix}, \quad \mathbf{w} = \begin{bmatrix} w_1 \\ w_3 \end{bmatrix}. \tag{33}$$

Thus, the expression derived in (25) yields to the CRB for the signal model in (28) once the redefinition in (33) is applied,

$$CRB_\tau = \frac{\mathrm{F_s} w_1}{2\mathrm{SNR}_{\text{out}}} \Bigg(\mathrm{F_s} \Re\left\{ \mathbf{qWq}^H \right\} - \frac{\mathrm{F_s} \Re\left\{ (\mathbf{qw})^H (\mathbf{qw}) \right\}^T}{w_1} \tag{34a}$$

$$+ \frac{\mathrm{F_s} \Im\left\{ (\mathbf{qw})^H (\mathbf{qw}) \right\}^T}{w_1 (1 + 2\sigma_{n_a}^2 \mathrm{SNR}_{\text{out}})} \Bigg)^{-1}. \tag{34b}$$

A similar assessment as in Section III can be conducted for (34). On the one hand, when $\sigma_{n_a}^2 \to \infty$ the term (34b) disappears to give way to the expression obtained in [17]. However, in this case, when $\sigma_{n_a}^2 \to \infty$, the resulting expression follows that of [20, Sec. 6.1], due to the fact that in this case the derivations considered a signal model with a compensated Doppler effect.

IV. Validation of the results

The aim of this section is to validate and analyse the CRB expressions obtained in (25) and (34), denoted as CRB_τ and CRB'_τ, respectively, for the time-delay τ parameter. It is worth noting that since the tests addressing the asymptotic estimation performance for the Doppler parameter b yielded the results already presented in [20], and earlier in [17], its assessment does not offer any additional contribution and was consequently excluded from this analysis. To provide contrast, three additional CRB expressions derived in previous studies

were also simulated and compared, as they offer valuable points of reference for comparison. On the one hand, the bound derived in [17], designated as $\mathrm{CRB}_{\tau}^{\mathrm{m}}$, employs a signal model that assumes full uncertainty regarding parameter ψ, and thus ϕ, leading to $\alpha \in \mathbb{C}$, as presented in (1). In this case, ψ is merged with the signal's amplitude α, converting it into a complex-valued parameter that accounts for changes in both sources, and which was estimated as a single entity. On the other hand, CRB_{τ}^{b} designates the bound in [19],

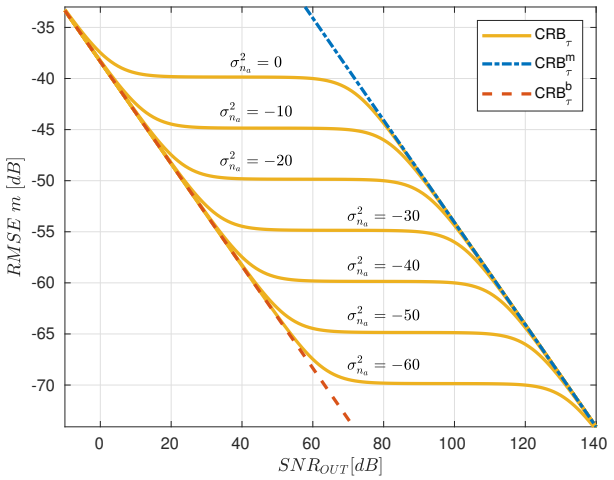

Fig. 1. CRB_{τ} in (25), tested for $\sigma^2_{n_a} = (-60, -50, \ldots, -10, 0)$ [dB]. CRB_{τ}^{b} and CRB_{τ}^{m} define the bounds for CRB_{τ}.

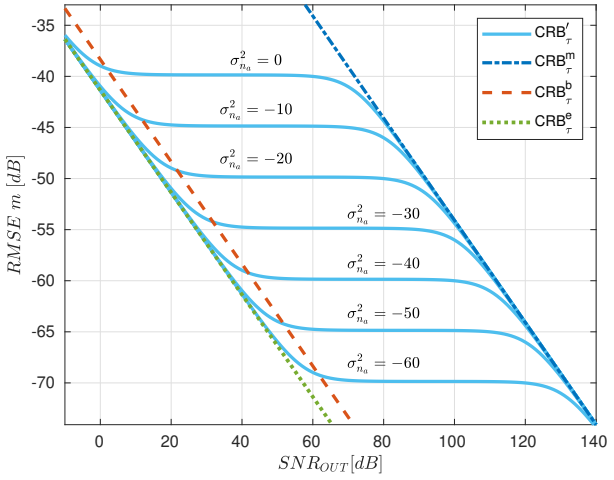

Fig. 2. CRB'_{τ} in (34), tested for $\sigma^2_{n_a} = (-60, \ldots, 0)$ [dB]. Now, CRB_{τ}^{e} and CRB_{τ}^{m} define the bounds for CRB_{τ}.

where ψ was assumed to be known and compensated for, enabling the incorporation of $w_c\tau$ into the signal model and subsequent derivations involved in the estimation performance assessment. Then, [20, Sec.6.1] provided a simplification of [19], yielding CRB_{τ}^{e}, by considering the Doppler effect b to be known and compensated. The perspectives offered

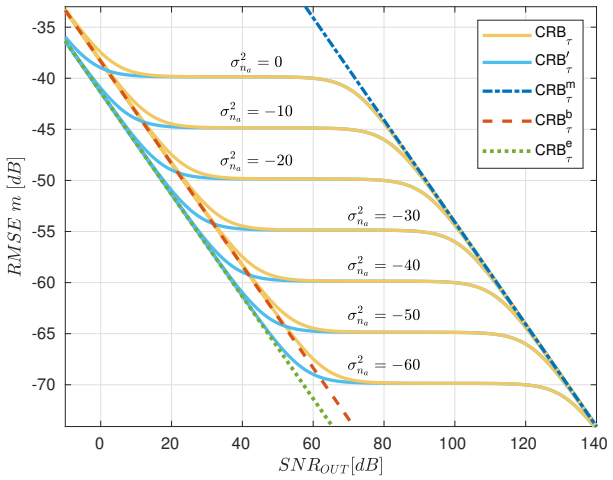

Fig. 3. CRB_{τ} in (25), and CRB'_{τ} in (34), tested for $\sigma^2_{n_a} = (-60, \ldots, 0)$ [dB]. Both curves overlap during the pleateau region and converge to CRB_{τ}^{m}. However, CRB_{τ} starts aligned with CRB_{τ}^{b}, whereas CRB'_{τ} to CRB_{τ}^{e}.

by these contributions are instrumental for this study. Note that, as $\sigma^2_{n_a}$ tends towards infinity, it implies nearly complete uncertainty in ψ, resembling the situation outlined in [17]. Conversely, as $\sigma^2_{n_a}$ decreases, ψ can be regarded as known, aligning more closely with the scenario depicted in [20].

To assess these perspectives, the testing setup utilized a GPS L1 C/A signal [5], which is composed by a periodic Gold CDMA sequence of 1023 chips modulated by a Binary Phase Shift Keying (BPSK) at a carrier frequency $\mathrm{F_c}$. An integration time of 1ms was set, together with a Doppler effect of 500Hz. The simulations were conducted for a set of 7 different values of $\sigma^2_{n_a}$ ranging from -60dB to 0dB, in steps of 10dB. These represent the level of confidence in the estimation of ψ, which affect both expressions in (25) and (34).

The results of the simulations are shown in figures 1 to 3. On the one side, figure 1 shows the RMSE provided by CRB_{τ} as a function of the $\mathrm{SNR_{out}}$, for the mentioned set of $\sigma^2_{n_a}$ values. In addition, it includes CRB_{τ}^{b} and CRB_{τ}^{m} for comparison. A foremost remark is that every CRB_{τ} behavior for each $\sigma^2_{n_a}$ choice can be categorized into three distinct regions: initially following CRB_{τ}^{b}, next plateauing with zero slope, and finally aligning with CRB_{τ}^{m}. In the first region, all CRB_{τ} RMSE values align with CRB_{τ}^{b}. As $\sigma^2_{n_a}$ increases, CRB_{τ} deviates earlier from CRB_{τ}^{b} to form a plateau, which persists until $\mathrm{SNR_{out}}$ values allow CRB_{τ} to converge to CRB_{τ}^{m}. This phenomenon validates the expression obtained for CRB_{τ} as it shows the anticipated behavior when examining the limits of (25) in Section III. At low $\mathrm{SNR_{out}}$, the impact of (25b) becomes more influential, resulting in an expression for CRB_{τ} similar to CRB_{τ}^{b}. Conversely, as SNRout increases, $\sigma^2_{n_a}$ becomes more negligible, leading CRB_{τ} to behave like CRB_{τ}^{m}.

A similar assessment to that provided in figure 1 can be done for figure 2. In this case, since the Doppler effect b was assumed to be known and compensated, CRB'_τ denotes lower RMSE at earlier $\mathrm{SNR}_{\mathrm{out}}$ values, compared to CRB_τ. In other words, CRB'_τ aligns with CRB^e_τ in the first region, which is located at lower MSE values than CRB^b_τ. This phenomenon was similarly noted in [20, Sec. 7], where it was attributed to the incorporation of additional information into the signal model, resulting in an reduction of approximately 6dB in the RMSE for any value of $\mathrm{SNR}_{\mathrm{out}}$.

Finally, in figure 3, a comparison is made between CRB'_τ and CRB_τ, revealing that while CRB'_τ initially aligns with CRB^e_τ at lower RMSE values, the plateau regions occur at the same RMSE level as that of CRB_τ for any $\sigma^2_{n_a}$ value selected.

V. Conclusion

Optimal time-delay assessments are frequently constrained by an unknown phase term due to transmitter-receiver misalignment in the antenna center of phases. This paper introduces a model treating this term as a stochastic variable, mirroring the measurement process undertaken by a sensor with a limited degree of precision. Time-delay and Doppler estimation performance is evaluated via the derivation of the CRB for two scenarios: a general signal model affected by the Doppler effect, and a static scenario without Doppler. Testing across various uncertainty levels associated with the unknown phase term, as a function of the receiver's SNR, reveals no novel findings for the Doppler effect compared to results obtained in previous contributions. Conversely, in the case of the time-delay parameter, three operation regions are observed. Firstly, the CRBs align with two associated reference bounds. Such reference bounds were derived in previous studies under the assumption of perfect knowledge on the antenna phase offset. Secondly, both CRBs form an almost zero-slope plateau. Lastly, they converge to a common reference bound, which was derived in a previous contribution and assumed complete uncertainty in the mentioned phase term. Notably, the CRB from the case disregarding the Doppler effect initially aligns with the reference bound at around 6dB lower error level. However, the second region shows that the error level for both CRBs is primarily determined by the uncertainty in the phase offset, for a wider range of SNR values. This underscores the critical role of sensor calibration for measuring such unknown phase term for improved performance.

References

[1] H. L. Van Trees, "Radar-sonar signal processing and gaussian signals in noise," *(No Title)*, 2001.

[2] J. Chen, Y. Huang, and J. Benesty, "Time delay estimation," *Audio signal processing for next-generation multimedia communication systems*, pp. 197–227, 2004.

[3] B. C. Levy, *Principles of signal detection and parameter estimation*. Springer Science & Business Media, 2008.

[4] E. D. Kaplan, Ed., *Understanding GPS: principles and applications*, 2nd ed. Artech House, 2006.

[5] P. J. G. Teunissen and O. Montenbruck, Eds., *Handbook of Global Navigation Satellite Systems*. Switzerland: Springer, 2017.

[6] D. A. Swick, "A Review of Wideband Ambiguity Functions," Naval Res. Lab., Washington DC, Tech. Rep. 6994, 1969.

[7] H. L. Van Trees, *Optimum Array Processing*. Wiley-Interscience, New-York, 2002.

[8] U. Mengali and A. N. D'Andrea, *Synchronization Techniques for Digital Receivers*. New York, USA: Plenum Press, 1997.

[9] S. M. Kay, *Fundamentals of Statistical Signal Processing: Estimation Theory*. Englewood Cliffs, New Jersey, USA: Prentice-Hall, 1993.

[10] P. Stoica and A. Nehorai, "Performances study of conditional and unconditional direction of arrival estimation," *IEEE Trans. Acoust., Speech, Signal Process.*, vol. 38, no. 10, pp. 1783–1795, Oct. 1990.

[11] A. Renaux, P. Forster, E. Chaumette, and P. Larzabal, "On the high-SNR conditional maximum-likelihood estimator full statistical characterization," *IEEE Trans. Signal Process.*, vol. 54, no. 12, pp. 4840 – 4843, Dec. 2006.

[12] H. L. Van Trees, *Detection, Estimation, and Modulation Theory, Part III: Radar – Sonar Signal Processing and Gaussian Signals in Noise*. J. Wiley & Sons, 2001.

[13] Q. Jin, K. M. Wong, and Z.-Q. Luo, "The Estimation of Time Delay and Doppler Stretch of Wideband Signals," *IEEE Trans. Signal Process.*, vol. 43, no. 4, p. 904–916, April 1995.

[14] A. Dogandzic and A. Nehorai, "Cramér-Rao bounds for estimating range, velocity, and direction with an active array," *IEEE Trans. Signal Process.*, vol. 49, no. 6, pp. 1122–1137, June 2001.

[15] N. Noels, H. Wymeersch, H. Steendam, and M. Moeneclaey, "True Cramér-Rao bound for timing recovery from a bandlimited linearly modulated waveform with unknown carrier phase and frequency," *IEEE Trans. on Communications*, vol. 52, no. 3, pp. 473–483, March 2004.

[16] Y. S. W. He-Wen and W. Qun, "Influence of random carrier phase on true cramér-rao lower bound for time delay estimation," in *Proc. of the IEEE Intl. Conf. on Acoustics, Speech and Signal Processing (ICASSP)*, Honolulu, USA, April 2007.

[17] D. Medina, L. Ortega, J. Vilà-Valls, P. Closas, F. Vincent, and E. Chaumette, "Compact CRB for Delay, Doppler, and Phase Estimation – Application to GNSS SPP and RTK Performance Characterisation," *IET Radar, Sonar & Navigation*, vol. 14, no. 10, pp. 1537–1549, 2020.

[18] P. Das, J. Vilà-Valls, E. Chaumette, F. Vincent, L. Davain, and S. Bonnabel, "On the accuracy limit of time-delay estimation with a band-limited signal," in *Proc. of the IEEE Intl. Conf. on Acoustics, Speech and Signal Processing (ICASSP)*, Brighton, UK, May 2019.

[19] J. M. Bernabeu, L. Ortega, A. Blais, Y. Gregoire, and E. Chaumette, "Time-delay and doppler estimation with a carrier modulated by a band-limited signal," in *2023 IEEE 9th International Workshop on Computational Advances in Multi-Sensor Adaptive Processing (CAMSAP)*, 2023, pp. 346–350.

[20] J. M. Bernabeu, L. Ortega, A. Blais, Y. Grégoire, and E. Chaumette, "On the asymptotic performance of time-delay and doppler estimation with a carrier modulated by a band-limited signal," *EURASIP - JASP*, 2023, article ID 295029. DOI: 10.21203/rs.3.rs-3539143/v1.

[21] C. Lubeigt, L. Ortega, J. Vilà-Valls, L. Lestarquit, and E. Chaumette, "Joint delay-doppler estimation performance in a dual source context," *Remote Sensing*, vol. 12, no. 23, 2020.

[22] H. McPhee, L. Ortega, J. Vilà-Valls, and E. Chaumette, "Accounting for acceleration—signal parameters estimation performance limits in high dynamics applications," *IEEE Transactions on Aerospace and Electronic Systems*, vol. 59, no. 1, pp. 610–622, 2023.

[23] C. Lubeigt, L. Ortega, J. Vilà-Valls, and E. Chaumette, "Untangling first and second order statistics contributions in multipath scenarios," *Signal Processing*, vol. 205, p. 108868, 2023.

[24] P. Das, L. Ortega, J. Vilà-Valls, F. Vincent, E. Chaumette, and L. Davain, "Performance limits of gnss code-based precise positioning: Gps, galileo & meta-signals," *Sensors*, vol. 20, no. 8, p. 2196, 2020.

[25] P. Stoica and Y. Selen, "Model-order selection: a review of information criterion rules," *IEEE Signal Processing Magazine*, vol. 21, no. 4, pp. 36 – 47, July 2004.

[26] D. Slepian, "Estimation of signal parameters in the presence of noise," *Transactions of the IRE Professional Group on Information Theory*, vol. 3, no. 3, pp. 68–89, 1954.

[27] G. A. F. Seber, *Matrix Handbook for Statisticians*. Wiley Series in Probability and Statistics, 2008.

[28] C. Shannon, "Communication in the presence of noise," *Proceedings of the IRE*, vol. 37, no. 1, pp. 10–21, 1949.